

Interplay of Coulomb repulsion and spin-orbit coupling in superconducting 3D quadratic band touching Luttinger semimetals

Serguei Tchoumakov¹, Louis J. Godbout¹, and William Witczak-Krempa^{1,2,3}

¹ Département de Physique, Université de Montréal, Montréal, Québec, H3C 3J7, Canada

serguei.tchoumakov@umontreal.ca

² Centre de Recherches Mathématiques, Université de Montréal; P.O. Box 6128, Centre-ville Station; Montréal (Québec), H3C 3J7, Canada

³ Regroupement Québécois sur les Matériaux de Pointe (RQMP)

Abstract. We investigate the superconductivity of 3D Luttinger semimetals, such as YPtBi, where Cooper pairs are constituted of spin-3/2 quasiparticles. Various pairing mechanisms have already been considered for these semimetals, such as from polar phonons modes, and in this work we explore pairing from the screened electron-electron Coulomb repulsion. In these materials, the small Fermi energy and the spin-orbit coupling strongly influence how charge fluctuations can mediate pairing. We find the superconducting critical temperature as a function of doping for an s -wave order parameter, and determine its sensitivity to changes in the dielectric permittivity. Also, we discuss how order parameters other than s -wave may lead to a larger critical temperature, due to spin-orbit coupling.

Keywords: superconductivity, Luttinger semimetals, Coulomb repulsion, critical temperature, Eliashberg equation, spin-orbit

1 Introduction

In regular metals, Coulomb repulsion is commonly believed to compete against the superconducting pairing between electrons. For example, in the electron-phonon mechanism of superconductivity with electron-phonon coupling g , the critical temperature below which an electron gas becomes superconducting is [1]

$$T_c = \frac{\langle\omega\rangle}{1.2} \exp\left(-\frac{1.04(1+\lambda)}{\lambda - \mu^*(1+0.62\lambda)}\right), \quad (1)$$

where $\lambda = 2 \int_0^\infty d\omega g^2 D(\omega)/\omega$ is the coupling constant, $\langle\omega\rangle = 2 \int_0^\infty d\omega g^2 D(\omega)$ is the averaged phonon frequency and μ^* is the Coulomb pseudo-potential. $D(\omega)$ is the phonon density of states. Eq. (1) informs us that increasing the electronic Coulomb repulsion exponentially decreases the critical temperature. In a normal electron gas, this strength is measured by the Wigner-Seitz radius

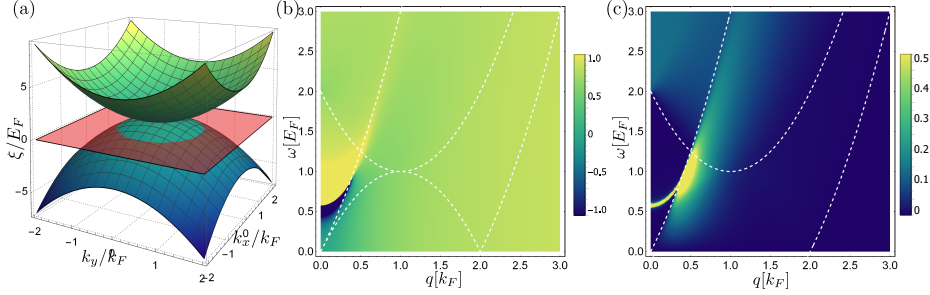


Fig. 1. (a) Band-structure of a Luttinger semimetal, the red plane is at the Fermi level. The upper and lower bands are doubly degenerate. (b-c) The (b) real and (c) imaginary parts of the inverse dielectric permittivity, $1/\epsilon(\omega, q)$, for $r_s = 0.5$ as a function of wavevectors, q , and frequencies, ω . The white dashed lines are the branches of the particle-hole continuum.

$r_s \approx 2me^2/\epsilon^*k_F$ where m is the band mass, e the electronic charge, ϵ^* the background dielectric constant and k_F is the Fermi wavevector. The superconductivity in semiconductors is often attributed to the electron-phonon coupling. However, for some materials such as SrTiO₃ and bismuth-based half-Heuslers, like YPtBi, the importance of the electron-phonon coupling in superconductivity is yet unresolved. In SrTiO₃ it was even proposed that superconductivity may come from the electron-electron repulsion [2,3]. The qualitative explanation does not only rely on the Kohn-Luttinger mechanism [4] but also on the contribution of plasmons to screening [2]. The effective attraction between electrons is a consequence of the screening of the Coulomb potential, with a dielectric function $\epsilon(\omega, \mathbf{q})$ that is computed in the random phase approximation

$$\epsilon_{\text{RPA}}(\omega, \mathbf{q}) = 1 - V_0(q)\Pi_0(\omega, \mathbf{q}), \quad (2)$$

with $V_0(q) = 4\pi e^2/(\epsilon^*q^2)$ the bare Coulomb potential and $\Pi_0(\omega, \mathbf{q})$ the bare electron polarisability. The dielectric function $\epsilon(\omega, \mathbf{q})$ depends on the system under study and has a role similar to the density of states of phonons, $D(\omega)$ that appears in Eq. (1). In Ref. [8] we use a variational approach similar to that in [5] to show how the critical temperature depends on each component (ω, \mathbf{q}) of the dielectric function, as we discuss further below.

This mechanism for SrTiO₃ however does not directly apply to bismuth-based half-Heusler materials, such as YPtBi, where the band structure is not well approximated by the free Hamiltonian $H_N(\mathbf{k}) = \hbar^2 k^2/(2m) - \mu$ but also includes strong spin-orbit coupling. It is a candidate Luttinger semimetal with Hamiltonian [6]

$$\hat{H}_0(\mathbf{k}) = \frac{\hbar^2}{2m} \left[-\frac{5}{4}\mathbf{k}^2 + (\mathbf{k} \cdot \hat{\mathbf{J}})^2 \right] - \mu, \quad (3)$$

where we introduce the $j = 3/2$ total angular momentum operators $\hat{\mathbf{J}} = (\hat{J}_x, \hat{J}_y, \hat{J}_z)$ and the chemical potential μ . This model has inversion, rotational and time-

reversal symmetries. The spectrum consists of four bands that meet quadratically at $\mathbf{k} = 0$ with degenerate lower and upper bands with energies $\pm \hbar^2 k^2 / (2m)$ as shown in Fig. 1(a). In the present proceeding we outline our findings regarding screening, quasiparticles and superconductivity in Luttinger semimetals arising from the screened Coulomb repulsion [7,8]. We also discuss how the $J = L = S = 1$ order parameter may have a larger critical temperature than in the s -wave channel, due to spin-orbit coupling.

2 Screening and electronic properties of Luttinger semimetals

We perturb the bare Hamiltonian (3) with the bare Coulomb potential $V_0(q)$

$$\hat{H}_{\text{int}} = \frac{1}{2\mathcal{V}} \sum_{s_1 s_2 \mathbf{k}_1 \mathbf{k}_2, \mathbf{q} \neq 0} V_0(q) \hat{\psi}_{\mathbf{k}_1 + \mathbf{q} s_1}^\dagger \hat{\psi}_{\mathbf{k}_2 - \mathbf{q} s_2}^\dagger \hat{\psi}_{\mathbf{k}_2 s_2} \hat{\psi}_{\mathbf{k}_1 s_1}, \quad (4)$$

where \mathcal{V} is the volume of the electron gas and introduce the annihilation operators $\hat{\psi}_{\mathbf{p}s} = \{\hat{\psi}_{\mathbf{p},3/2}, \hat{\psi}_{\mathbf{p},1/2}, \hat{\psi}_{\mathbf{p},-1/2}, \hat{\psi}_{\mathbf{p},-3/2}\}$ of the aforementioned $j = 3/2$ representation. In the following, we set $\hbar = k_B = 1$ with energies in units of the Fermi energy E_F and wavevectors in units of the Fermi wavevector k_F . The amplitude of the Coulomb potential is then given by the Wigner-Seitz radius, $r_s = me^2 / (\alpha \epsilon^* k_F)$ with $\alpha \approx 0.51$. In [7] we computed the bare charge polarisability $\Pi_0(\omega, \mathbf{q})$ and the self-energy corrections $\Sigma_{\pm}(\omega, \mathbf{k})$ on the upper (+) and lower (−) bands. We find that, because of strong spin-orbit coupling, the plasma frequency is diminished compared to a regular quadratic band, and that screening receives important contributions from interband excitations (see Figs. 1(b,c)).

The difference in screening between a Luttinger semimetal and a normal electron gas affects the quasiparticle properties. We find that for Luttinger semimetals the quasi-particle residue Z_F and the first Landau coefficients, f_{0s} and f_{1s} , are less affected by the Coulomb potential [7].

3 Superconductivity in Luttinger semimetals

We evaluate the critical temperature of a singlet s -wave superconductor using the linear Eliashberg equation [3,9], with account of self-energy corrections,

$$\lambda(T) \phi_{\sigma_1}(i\omega_{n_1}, k_1) = -T \sum_{\sigma_2 \omega_{n_2}} \int_0^\infty dk_2 \frac{k_2}{k_1} \frac{I_{0\sigma_1\sigma_2}(i\omega_{n_1}, k_1; i\omega_{n_2}, k_2) \phi_{\sigma_2}(i\omega_{n_2}, k_2)}{(\omega_{n_2} Z_{\sigma_2}(i\omega_{n_2}, k_2))^2 + (\xi_{\sigma_2}(k_2) + \chi_{\sigma_2}(i\omega_{n_2}, k_2))^2}, \quad (5)$$

where ϕ_σ represents the superconducting order parameter, $\omega_n = (2n+1)\pi T$ are the Matsubara frequencies, $\sigma = \pm$ is the band index, I_0 is the angular average of the screened Coulomb potential with spin-orbit corrections and $\Sigma_{\pm}(i\omega_n, k) \equiv \chi_{\pm}(i\omega_n, k) + i\omega_n(1 - Z_{\pm}(i\omega_n, k))$ are the self-energy corrections. Note that we have included the pairing order parameter on the upper band (+), as it will

play an important role. Eq. (5) is an eigenvalue equation where the critical temperature is found for eigenvalues $\lambda(T)$ such that $\lambda(T_c) = 1$.

In this approach, the absence of symmetry in Eq. (5) on parameters (σ, ω_n, k) makes its resolution complex and time consuming. We thus perform the transformation $\phi_\sigma(i\omega_n, k) \rightarrow \bar{\phi}_\sigma(i\omega_n, k) = k\phi_\sigma(i\omega_n, k)/((\omega_n Z_\sigma(i\omega_n, k))^2 + (\xi_\sigma(k) + \chi_\sigma(i\omega_n, k))^2)$ to have a symmetric form of Eq. (5)

$$\rho(T)\bar{\phi} = S\bar{\phi}, \quad (6)$$

with S a symmetric operator on parameters (σ, ω_n, k) and where the critical temperature T_c is obtained for $\rho(T_c) = 0$. One can show that $\rho(T > T_c) < 0$, so T_c is computed from the largest eigenvalue ρ^{\max} and, using the variational properties of symmetric matrices, for any test function $\bar{\phi}^t$:

$$\rho^{\max} \geq \rho^t = \frac{\bar{\phi}^t \cdot S\bar{\phi}^t}{\bar{\phi}^t \cdot \bar{\phi}^t} \Rightarrow T_c \geq T_c^t, \quad (7)$$

with T_c^t the critical temperature obtained with the test function.

We use this equation to reproduce the critical temperature for singlet s -wave pairing from the screened Coulomb repulsion in a single quadratic band structure [9], and compute it for a Luttinger semimetal (see Fig. 2). For large Wigner-Seitz radii, the critical temperature of the Luttinger semimetal $T_c/T_F \approx 4.4 \times 10^{-4}$ is smaller than for a single quadratic band, but extends to smaller values of r_s [8]. We note that it was important to keep ϕ_+ in Eq. (5), otherwise we would not find a solution. The value we obtain is comparable to the ratio $T_c/T_F \approx (2-5) \times 10^{-4}$ from measurements on the half-Heusler YPtBi [10,11,12]. Because we have an s -wave superconductor, our result stands in contradiction with a recent proposition that YPtBi is a line-node superconductor [13] but this interpretation, based on magnetic properties, is arguable due to the small value of the lower critical field B_{c1} in YPtBi [14], among other caveats.

Because the critical temperature depends on an integral equation involving every component $(i\Omega_n, q)$ of the dielectric function $\epsilon(i\Omega_n, q)$, it is not straightforward to understand the origin of superconductivity. If one changes $\epsilon(i\Omega_n, q)$ by $\delta\epsilon(i\Omega_n, q)$ then the critical temperature T_c changes by

$$\Delta T_c = 2\pi T \sum_{\Omega_n} \int dq \frac{\delta T_c}{\delta\epsilon(i\Omega_n, q)} \delta\epsilon(i\Omega_n, q). \quad (8)$$

The functional derivative $\delta T_c/\delta\epsilon(i\Omega_n, q)$ is a measure of the sensitivity of the critical temperature to screening. Here, the functional derivative can be decomposed into

$$\frac{\delta T_c}{\delta\epsilon(i\Omega_n, q)} = - \left. \frac{\delta\rho}{\delta\epsilon(i\Omega_n, q)} \right|_{T=T_c} \bigg/ \left. \frac{\partial\rho}{\partial T} \right|_{T=T_c}. \quad (9)$$

In this equation, ρ is the maximal eigenvalue of the linear Eliashberg equation (6). We use it to evaluate numerically the derivative $\partial\rho/\partial T|_{T=T_c}$ and we use the Hellmann-Feynman theorem to compute $\delta\rho/\delta\epsilon(i\Omega_n, q)$ [8]. In Fig. 2(b,c),

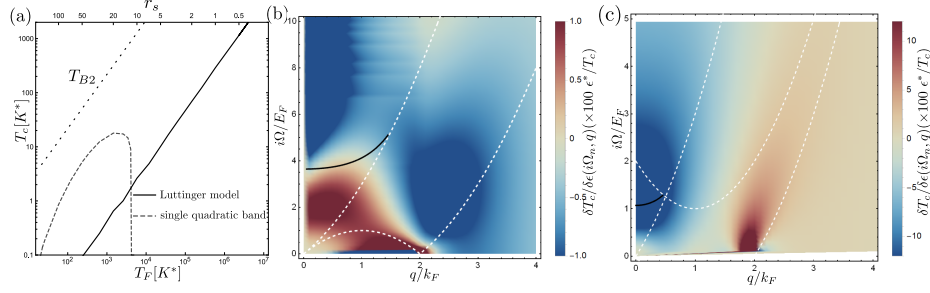


Fig. 2. (a) Critical temperature in units of $K^* = m/(m_e \epsilon^{*2})K$ for a single quadratic band (gray, dashed) and a Luttinger semimetal (plain, black). For comparison we superimpose the Bose-Einstein condensation temperature T_{B2} for a density $n/2$ and a mass $2m$. Reproduced with permission from [8]. (b-c) The functional derivative $\delta T_c / \delta \epsilon(i\Omega_n, q)$ in percent of the critical temperature for (b) a single quadratic band structure and (c) a Luttinger semimetal, for $r_s = 15$. The white dashed lines are the branches of the particle-hole excitation diagram in real frequency and the black line is the plasmon dispersion in real frequency. The critical temperature is mostly sensitive to the dielectric function in the region of plasmons and near the $q = 2k_F$ static screening.

we show the sensitivity of the critical temperature T_c to the different components of the dielectric function $\epsilon(i\Omega_n, q)$ for a quadratic band and a Luttinger semimetal [8]. We notice larger values in the area associated to plasmons and close to $2k_F$, which are respectively associated to plasmon and Kohn-Luttinger mechanisms of superconductivity [2,4].

4 Pairing beyond s -wave from spin-orbit coupling

In Luttinger semimetals, the quasiparticles are described with $j = 3/2$ multiplets instead of spin-1/2 as in ordinary metals. The rotational symmetry of Eqs. (3 - 4) allows to describe Cooper pairs by a gap function $\Delta^{J,LS}(i\omega_n, k)$ with a well defined total angular momentum J that combines the pseudo-spin S of the Cooper pair and its orbital angular momentum L [16,17]. At the critical temperature, these gap functions satisfy the linear Eliashberg equations

$$\lambda(T) \Delta_{\sigma_1}^{J, L_1 S_1}(i\omega_{n_1}, k_1) = -T \sum_{\substack{\ell \sigma_2 \omega_{n_2} \\ L_2 S_2}} \int \frac{dk_2 k_2}{k_1} \frac{V_\ell(i(\omega_{n_1} - \omega_{n_2}), k_1, k_2) A_{\ell, \sigma_1 \sigma_2}^{J, L_1 S_1 L_2 S_2}(k_1, k_2)}{(\omega_{n_2} Z_{\sigma_2}(i\omega_{n_2}, k_2))^2 + (\xi_{\sigma_2}(k_2) + \chi_{\sigma_2}(i\omega_{n_2}, k_2))^2} \Delta_{\sigma_2}^{J, L_2 S_2}(i\omega_{n_2}, k_2), \quad (10)$$

with $\lambda(T) = 1$ for $T = T_c$. Note that we have written the Eliashberg equation in its non-symmetrized form, in contrast to Eq. (6). This self-consistent relation can be complemented with off-diagonal components of the gap function [18], that we neglect in the present discussion. In Eq. (10), the electron pairing is determined by V_ℓ , the projection of the screened Coulomb potential $V_0(q)/\epsilon(i\Omega_n, \mathbf{q})$ on the

ℓ -th Legendre polynomial P_ℓ , and by the form factor due to spin-orbit coupling :

$$A_{\ell, \sigma_1 \sigma_2}^{J, L_1 S_1 L_2 S_2} = \frac{2\ell + 1}{2} \int \frac{d^2 \Omega_1 d^2 \Omega_2}{(2\pi)^3} P_\ell(\hat{\mathbf{k}}_1 \cdot \hat{\mathbf{k}}_2) \text{Tr}[\hat{P}_{\sigma_1}(\mathbf{k}_1) \hat{N}^{J, L_1 S_1}(\mathbf{k}_1) \hat{P}_{\sigma_2}(\mathbf{k}_2) \hat{N}^{J, L_2 S_2 \dagger}(\mathbf{k}_2)], \quad (11)$$

where Ω_i is the solid angle of \mathbf{k}_i . Here, the matrices $\hat{N}^{J, LS}(\mathbf{k})$ correspond to the representation of the rotation symmetry on $\mathbf{J} = \mathbf{L} + \mathbf{S}$,

$$\hat{N}^{J, LS}(\mathbf{k}) = \sum_{m_L m_S} C_{L m_L, S m_S}^J Y_{L m_L}(\theta_{\mathbf{k}}, \phi_{\mathbf{k}}) \hat{M}_{S m_S} \quad (12)$$

where $C_{L m_L, S m_S}^J$ are the Clebsch-Gordan coefficients, $Y_{L m_L}$ the spherical harmonics and $\hat{M}_{S m_S}$ the pairing matrices with pseudo-spin S of the Cooper pairs. Some of these combinations, for $L = 0, 1$, are listed in [16,17]. We introduce the projectors \hat{P}_\pm in Eq. (11) to decompose the gap equation on the eigenstates of \hat{H}_0 on the upper (+) and lower (−) bands, that we respectively associate to eigenstates $\pm 3/2$ and $\pm 1/2$ of the helicity operator $\hat{\lambda} = \hat{\mathbf{k}} \cdot \hat{\mathbf{J}}$. Note that, for a given value of J , there is a finite number of components V_ℓ that contribute in the summation in Eq. (10). For example, for s -wave $J = L = S = 0$ only $\ell = 0$ and 2 contribute. In the following, we further simplify Eq. (10) by considering a gap function in a unique (J, L, S) sector, $\Delta^{J, LS}$, and write $A_{\ell, \sigma_1 \sigma_2}^{J, L S L S} = A_{\ell, \sigma_1 \sigma_2}^{J, LS}$. A more refined analysis would allow for mixing between different values of (L, S) for a fixed J .

It is expected that the amplitude of the pairing potential depends on the largest combination of the coefficients V_ℓ and $A_{\ell, \sigma_1 \sigma_2}^{J, LS}$ close the Fermi surface, where $\sigma_1 = \sigma_2 = -$ and $k_1 = k_2 = k_F$. To be more accurate, one should consider the full k -dependence but let us work in this simpler limit. It was shown that this amplitude is the strongest for $J = L = S = 0$ [16], which is precisely the order parameter we consider in our work (see section 3). This logic of maximizing the product $V_\ell A_{\ell, \sigma_1 \sigma_2}^{J, LS}$ applies well for superconductivity from an attractive potential, like the electron-phonon coupling, where the eigenvalue of Eq. (10) with the largest absolute value, $\lambda_1(T)$, is already positive. However, it is not straightforward to extend to superconductivity from a repulsive potential, such as the Coulomb repulsion between electrons, where in the s -wave channel the eigenvalue with the largest absolute value is negative, $\lambda_1(T) < 0$, because of the overall repulsive nature of the Coulomb potential. Then, the s -wave solution to Eq.(10) comes from the second largest-in-absolute-value eigenvalue, $\lambda_2(T) > 0$, which corresponds to the first electronic configuration where the Coulomb potential is attractive [9].

Naively, the interband coupling may seem unfavoured due to the difference in energy between the two bands but it is worth considering its contribution. Indeed, we find that for $J = L = S = 1$, *i.e.* $\hat{N}^{111} = \sqrt{3}(-k_z(\hat{J}_x + i\hat{J}_y) + (k_x + ik_y)J_z)/(\sqrt{5}k)$ [16], the coupling is non-zero only for $\ell = 1$ and decomposes as a matrix on the bands with helicity $\pm 1/2$ and $\pm 3/2$:

$$A_1^{111} = \begin{pmatrix} 2/5 & 3/10 \\ 3/10 & 0 \end{pmatrix}. \quad (13)$$

This matrix has eigenvalues $(2 \pm \sqrt{13})/10$. Interestingly, one of them is negative (≈ -0.16) and thus, for the corresponding configuration of the gap function on the upper and lower bands, the eigenvalue $\lambda_1(T)$ with the largest absolute value can be positive instead of negative. This way, due to the difference in magnitude between $\lambda_1(T)$ and $\lambda_2(T)$, it may be possible to obtain a larger critical temperature with $J = L = S = 1$ (where $|\lambda_1| > |\lambda_2|$ and $\lambda_1 > 0$) than for $J = L = S = 0$ (where $|\lambda_1| > |\lambda_2|$ but $\lambda_1 < 0$). However, for this to happen, the amplitude of the Coulomb repulsion has to overcome the difference in energy between the two bands and a more refined study is needed to evaluate the corresponding critical temperature.

5 Conclusion

Over a wide range of doping, we find that the s -wave critical temperature for a Luttinger semimetal with screened Coulomb repulsion is $T_c/T_F \approx 4.4 \times 10^{-4}$. T_c/T_F is small but may be an explanation for the superconductivity of YPtBi, a candidate Luttinger semimetal, where experiments report $T_c/T_F \approx (1-8) \times 10^{-4}$. Previous theoretical works on YPtBi, with phonon-based pairing, estimate a critical temperature at least one order of magnitude smaller than in experiments [16,19]. We quantitatively show the origins of superconductivity, in relation to the plasmon [9] and Kohn-Luttinger [4] mechanisms of superconductivity. We also analyze the Eliashberg equation of $j = 3/2$ fermions [16,17] and propose that an unconventional order parameter, with $J = L = S = 1$, may turn the repulsive contribution of the screened Coulomb potential to attractive. This reminds a recent discussion on graphene, where the Berry curvature promotes the $\ell = 1$ component of a repulsive interaction to attractive [20]. A more involved study would be required to determine the dominant superconducting channel.

Acknowledgments. This project is funded by a grant from Fondation Courtois, a Discovery Grant from NSERC, a Canada Research Chair, and a “Établissement de nouveaux chercheurs et de nouvelles chercheuses universitaires” grant from FRQNT. This research was enabled in part by support provided by Calcul Québec (www.calculquebec.ca) and Compute Canada (www.computecanada.ca).

References

1. McMillan, W. L. : Transition Temperature of Strong-Coupled Superconductors. Phys. Rev. 167 2 331-334 (1968). doi:10.1103/PhysRev.167.331
2. Y. Takada : Theory of Superconductivity in Polar Semiconductors and Its Application to N-Type Semiconducting SrTiO₃. Journal of the Physical Society of Japan 49 4 1267-1275 (1980). doi:10.1143/JPSJ.49.1267
3. J. Ruhman and P. A. Lee : Superconductivity at very low density: The case of strontium titanate. Phys. Rev. B 94 22 224515 (2016). doi:10.1103/PhysRevB.94.224515
4. W. Kohn and J.M. Luttinger : New Mechanism for Superconductivity. Phys. Rev. Lett. 15 12 524-526 (1965). doi:10.1103/PhysRevLett.15.524

5. P.B. Allen and R.C. Dynes : Transition temperature of strong-coupled superconductors reanalyzed. *Phys. Rev. B* 12 3 905-922 (1975). doi:10.1103/PhysRevB.12.905
6. J.M. Luttinger : Quantum Theory of Cyclotron Resonance in Semiconductors: General Theory. *Phys. Rev.* 102 4 1030-1041 (1956). doi:10.1103/PhysRev.102.1030
7. S. Tchoumakov and W. Witczak-Krempa : Dielectric and electronic properties of three-dimensional Luttinger semimetals with a quadratic band touching. *Phys. Rev. B* 100 7 075104 (2019). doi:10.1103/PhysRevB.100.075104
8. S. Tchoumakov, L. J. Godbout and W. Witczak-Krempa : Superconductivity from Coulomb repulsion in three-dimensional quadratic band touching Luttinger semimetals. arXiv:1910.04189. <https://arxiv.org/abs/1910.04189>
9. Y. Takada : Plasmon Mechanism of Superconductivity in the Multivalley Electron Gas. *Journal of the Physical Society of Japan* 61 238-253 (1992). doi:10.1143/JPSJ.61.238
10. N. P. Butch, P. Syers, K. Kirshenbaum, A. P. Hope, and J. Paglione : Superconductivity in the topological semimetal YPtBi. *Phys. Rev. B* 84, 220504(R) (2011). doi:10.1103/PhysRevB.84.220504
11. T. V. Bay, T. Naka, Y. K. Huang, and A. de Visser : Superconductivity in noncentrosymmetric YPtBi under pressure. *Phys. Rev. B* 86, 064515 (2012). doi:10.1103/PhysRevB.86.064515
12. C. Shekhar, M. Nicklas, A. K. Nayak, S. Ouardi, W. Schnelle, G. H. Fecher, C. Felser and K. Kobayashi : Electronic structure and nonsaturating magnetoresistance of superconducting Heusler topological insulators. *Journal of Applied Physics* 113, 17E142 (2013). doi:10.1063/1.4799144
13. H. Kim, K. Wang, Y. Nakajima, R. Hu, S. Ziemak, P. Syers, L. Wang, H. Hodovanets, J. D. Denlinger, P. M. R. Brydon, D. F. Agterberg, M. A. Tanatar, R. Prozorov and J. Paglione : Beyond triplet: Unconventional superconductivity in a spin-3/2 topological semimetal. *Science Advances* 4, 4 (2018). doi:10.1126/sciadv.aao4513
14. T.V. Bay, M. Jackson, C. Paulsen, C. Baines, A. Amato, T. Orvis, M.C. Aronson, Y.K. Huang and A. de Visser : Low field magnetic response of the non-centrosymmetric superconductor YPtBi. *Solid State Communications* 183, 13-17 (2014). doi:10.1016/j.ssc.2013.12.010
15. E. Langmann : Theory of the upper critical magnetic field without local approximation. *Physica C: Superconductivity* 159, 5 561-569 (1989). doi:10.1016/0921-4534(89)91286-0
16. Lucile Savary, Jonathan Ruhman, Jrn W. F. Venderbos, Liang Fu, and Patrick A. Lee : Superconductivity in three-dimensional spin-orbit coupled semimetals. *Phys. Rev. B* 96, 214514 (2017). doi:10.1103/PhysRevB.96.214514
17. Bitan Roy, Sayed Ali Akbar Ghorashi, Matthew S. Foster, and Andriy H. Nevidomskyy : Topological superconductivity of spin-3/2 carriers in a three-dimensional doped Luttinger semimetal. *Phys. Rev. B* 99, 054505 (2019). doi:10.1103/PhysRevB.99.054505
18. M Smidman, M B Salamon, H Q Yuan and D F Agterberg : Superconductivity and spinorbit coupling in non-centrosymmetric materials: a review. *Rep. Prog. Phys.* 80 036501 (2017). doi:10.1088/1361-6633/80/3/036501
19. Markus Meinert : Unconventional Superconductivity in YPtBi and Related Topological Semimetals. *Phys. Rev. Lett.* 116, 137001 (2016). doi:10.1103/PhysRevLett.116.137001
20. Tommy Li, Julian Ingham, Harley D. Scammell : Unconventional Superconductivity in Semiconductor Artificial Graphene. arXiv:1909.07401 (2019). <https://arxiv.org/abs/1909.07401>